drogen atoms were placed in calculated positions (C–H = 0.95 Å) and were constrained to ride on their respective carbon atoms.

The absolute configuration was assigned by first assuming the *R,R* configuration. Six final cycles of least-squares refinement converged at $R_1 = 0.0448$ and $R_2 = 0.0493$. Anomalous dispersion due to Mo was included in the calculation. The alternate hand of the structure was then refined to convergence from the same starting point, again with six cycles of least-squares refinement, giving a final $R_1 = 0.0466$ and $R_2 = 0.0515$. Thus the original assignment of configuration, depicted in Figure 1, was shown to be correct.

Crystal data: $a = 6.881$ (3) Å, $b = 12.679$ (2) Å, $c = 20.176$ (4) Å, $\beta = 92.03$ (3)°, $V = 1759.1$ Å^3, space group = $P2_1$, $Z = 4$, $M_r = 377.3$, ρ(calcd) = 1.425 g cm^{-3}, $\mu = 7.2$ cm^{-1}. A semiempirical absorption correction was applied. Figure 1 shows the geometry of **5a** and **5b** along with the atomic numbering scheme. Table II shows selected bond distances and angles.

Acknowledgment. We thank the National Science Foundation for financial support (Grant CHE-8308355). We also thank the Biomedical Research Support-Shared Instrumentation Grant Program, Division of Research Resources, for funds to purchase the X-ray diffraction equipment (NIH Grant S10RR02243-01). J.M.H. thanks the Fannie and John Hertz Foundation for a graduate fellowship (1982–1985).

Registry No. (*R,R*)-**1**, 100994-70-5; **2**, 100994-71-6; **4**, 100994-68-1; **5**, 101053-54-7; **6**, 101053-55-8; **7**, 100994-69-2; $MoO_2(acac)_2$, 17524-05-9; *t*-BuCHO, 630-19-3; 2,6-dibromopyridine, 626-05-1; 2,6-dibromopyridine *N*-oxide, 25373-69-7.

Supplementary Material Available: Listings of final positional and thermal parameters and final observed and calculated structure factors (24 pages). Ordering information is given on any current masthead page.

Contribution from the Department of Chemistry
and Biochemistry, University of California at Los Angeles,
Los Angeles, California 90024

Single-Crystal Polarized Electronic Absorption Spectra and Ligand Field Parameters for the Trichloro(triethylphosphine)platinate(II) Ion

Julia R. Phillips and Jeffrey I. Zink*

Received August 1, 1985

The bonding properties of phosphine ligands have been studied by a variety of techniques. The most extensive studies have been IR spectroscopic investigations of changes in carbonyl stretching frequencies in phosphine–carbonyl compounds. In addition, NMR spectroscopy and X-ray crystallography have been used as the basis for discussion of σ- and π-bonding properties.

Electronic absorption spectroscopic measurements of the position of phosphine in the spectrochemical series are relatively scarce. The major factors contributing to the scarcity are the relatively high energies of the d–d bands, which frequently cause them to be obscured by charge-transfer bands, and the relatively large extinction coefficients, which make studies of single crystals difficult. Phosphine ligands have been studied the most extensively in tetrahedral Ni(II) and Co(II) complexes.[1-8] The results have indicated that phosphines are strong ligands in the spectrochemical series. Jørgensen has concluded that the triethylphosphine ligand "has a spectrochemical position slightly above the ammines."[9] Triphenylphosphine is a better σ donor and a better π acceptor than halides.[1]

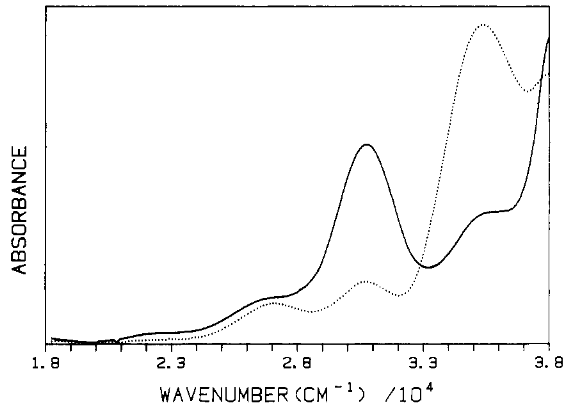

Figure 1. Single-crystal polarized electronic absorption spectrum of $(Pr_4N)[PtCl_3PEt_3]$ at room temperature. The two curves were obtained in orthogonal polarization directions.

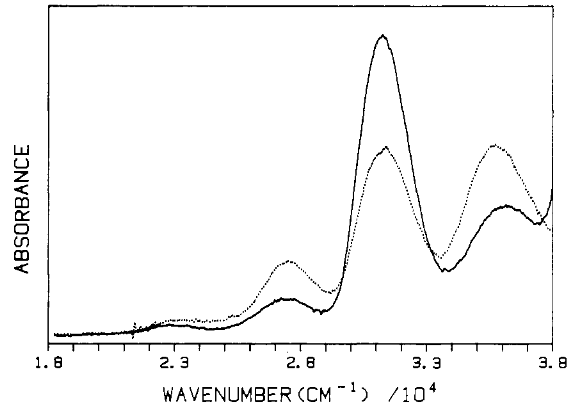

Figure 2. Single-crystal polarized electronic absorption spectrum of $(Pr_4N)[PtCl_3PEt_3]$ at 10 K. The two curves were obtained in orthogonal polarization directions.

A series of compounds that is proving amenable to detailed electronic spectroscopic study is the $PtCl_3L^{n-}$ series where the ligand L can range from "Werner" ligands such as ammines and halides[10-13] to ligands of interest in organometallic chemistry such as ethylenes, CO, and phosphines.[14-16] Microspectroscopic techniques allow measurements to be made on single crystals even when the extinction coefficients are greater than 10^3.[14] We report here the low-temperature single-crystal polarized electronic absorption spectra of $PtCl_3PEt_3^-$ and the angular overlap ligand field analysis of the σ and π interactions with the metal d orbitals.

Experimental Section

$(Pr_4N)[PtCl_3PEt_3]$ was prepared according to the method of Duddell et al.[17] Single crystals were grown between quartz plates that were stored in a covered dish. A drop of a solution of the complex in chloroform was put onto one plate, and a second plate was pressed on top of the first. The dish was covered and allowed to stand for several hours

---

(1) (a) Davies, J. E.; Gerloch, M.; Phillips, D. J. *J. Chem. Soc., Dalton Trans.* **1979**, 1836. (b) Gerloch, M.; Hanton, L. R. *Inorg. Chem.* **1981**, *20*, 1046.

(2) Bertini, I.; Gatteschi, D.; Mani, F. *Inorg. Chem.* **1972**, *11*, 2464.

(3) (a) Flamini, A.; Sestili, L.; Furlani, C. *Inorg. Chim. Acta* **1971**, *5*, 241. (b) Tomlinson, A. A. G.; Bellitto, C.; Piovesana, O.; Furlani, C. *J. Chem. Soc., Dalton Trans.* **1972**, 350.

(4) Fereday, R. J.; Hathaway, B. J.; Dudley, R. J. *J. Chem. Soc. A* **1970**, 571.

(5) Chastain, B. B.; Rick, E. A.; Pruett, R. L.; Gray, H. B. *J. Am. Chem. Soc.* **1968**, *90*, 3994.

(6) Simo, C.; Holt, S. *Inorg. Chem.* **1968**, *7*, 2655.

(7) Hatfield, W. E.; Yoke, J. T. *Inorg. Chem.* **1962**, *1*, 475.

(8) Cotton, F. A.; Faut, O. D.; Goodgame, D. M. L.; Holm, R. H. *J. Am. Chem. Soc.* **1961**, *83*, 1780.

(9) Jørgensen, C. K. "Inorganic Complexes"; Academic Press: New York, 1963, p. 157.

(10) (a) Fenske, R. F.; Martin, D. S.; Ruedenberg, K. *Inorg. Chem.* **1962**, *1*, 441. (b) Fanwick, P. E.; Martin, D. S. *Inorg. Chem.* **1973**, *12*, 24.

(11) Franke, E.; Moncuit, C. *Theor. Chim. Acta* **1973**, *29*, 319.

(12) Tuszynski, W.; Gliemann, G. *Z. Naturforsch., A: Phys., Phys. Chem., Kosmophys.* **1979**, *34A*, 211.

(13) Vanquickenborne, L. G.; Ceulemans, A. *Inorg. Chem.* **1981**, *20*, 796.

(14) Chang, T.-H.; Zink, J. I. *J. Am. Chem. Soc.* **1984**, *106*, 287.

(15) Chang, T.-H.; Zink, J. I. *Inorg. Chem.* **1985**, *24*, 4499.

(16) Chang, T.-H. Ph.D. Dissertation, University of California, Los Angeles, 1984.

(17) Duddell, D. A.; Goggin, P. L.; Goodfellow, R. J.; Norton, M. G.; Smith, J. G. *J. Chem. Soc. A* **1970**, 545.

Table I. Calculated and Observed Transition Energies

transition energies, cm^{-1}		
calcd[a]	obsd	assignts
	Singlets	
31 264	31 300	$^1B_1$ ($d_{xy} \rightarrow d_{x^2-y^2}$)
35 882	35 700	$^1B_2$ ($d_{xz} \rightarrow d_{x^2-y^2}$)
36 124	36 200	$^1A_2$ ($d_{yz} \rightarrow d_{x^2-y^2}$)
40 503	*b*	...
	Triplets	
22 018		B_2
22 599		B_2
22 781	22 600	A_2
22 831		B_2
23 620		A_2
25 353		A_2
25 356	24 800 (sh)	B_1
25 385		B_2
27 316	27 600	B_1
28 655	28 300 (sh)	A_1
28 684		A_1
30 879	*c*	A_1

[a] Transition energies were calculated by using the following parameters (cm^{-1}): $e_\sigma = 11\,800$, $e_{\pi_\parallel} = 3000$, $e_{\pi_\perp} = 2700$, $e_\sigma = 23\,500$, $e_{\pi_\parallel} = 2500$, $e_{\pi_\perp} = 3000$, $e_{sd} = 17\,650$, $B = 690$, $C = 2850$, $\xi = 2850$. [b] The experimental spectrum does not extend to this region. The calculated energy includes s–d orbital mixing by using e_{sd}.[11,13,15] [c] Obscured by the $^1B_1$ band.

until crystals formed. Large, irregularly shaped crystals were obtained. The plates were separated, and the crystals were examined under a polarizing microscope to determine their thicknesses and their extinction properties. Crystals that appeared first-order gray that also had distinct extinction axes were selected for spectroscopic study. The requirement of ultrathin crystals for absorption spectroscopy precluded identification of both the crystal face and the projection of the electric vector of the radiation on the molecular axes. A locally constructed microspectrophotometer that has been described previously[14] was used to record the crystal spectra in two orthogonal polarizations along the crystal's extinction directions at both room temperature and 10 K.

Results

Figures 1 and 2 show polarized electronic absorption spectra of single crystals of $(Pr_4N)[PtCl_3PEt_3]$. The spectra in Figure 1 were obtained from a thin crystal at room temperature, while those in Figure 2 were obtained from a different thin crystal at 10 K. The energies of the peaks and shoulders are listed in Table I.

The observed bands fall into two categories, high-energy (>29 000 cm^{-1}) bands with extinction coefficients greater than 500 L/(M cm), and low-energy (<29 000 cm^{-1}) bands with extinction coefficients less than 200 L/(M cm). All bands show a red shift of several hundred reciprocal centimeters when the temperature is raised from 10 K to room temperature. The lowest of these high-energy bands occurs at 31 300 cm^{-1} in both polarizations, but with a lower intensity in the polarization indicated by the dotted line. This band is very symmetrical in both polarizations. The next band occurs at about 36 000 cm^{-1} with a higher intensity in the dotted-line polarization. There is an apparent red shift of the band in the polarization direction shown by the dotted line with respect to the band shown by the solid line. This apparent shift is caused by changing intensities of two overlapping bands. The highest energy component, observed at 36 200 cm^{-1} in the polarization indicated by the solid line, is clearly a different band from the one at 35 700 cm^{-1} observed in the orthogonal polarization direction.

The energies of the low-energy features were determined by using the spectra of a thick crystal. The lowest energy band occurs at 22 600 cm^{-1}. A distinct but unresolved shoulder is observed at 24 800 cm^{-1}. A more intense band is seen at 27 600 cm^{-1} with a shoulder at 28 100 cm^{-1}. This band is observed in both polarizations. The broadness of these bands, due to a distribution of triplet spin-forbidden transitions throughout the region, will be discussed below.

Discussion

Assignments of the Transitions. The solution spectrum of $(Pr_4N)[PtCl_3PEt_3]$ in dichloromethane gives bands at 282, 324, and 373 nm with extinction coefficients of 630, 510, and 160 L/(M cm), respectively. These bands correspond to the three most obvious bands in the single-crystal spectra. Bands with extinction coefficients in this range are typical of d–d transitions. Therefore, all of the transitions observed in the single-crystal spectra can be attributed to d–d transitions. Because of the similarity between these spectra and those found previously for other complexes of the type $PtCl_3L^{n-}$, the spin-allowed singlet d–d transitions are readily assigned in a manner consistent with the assignments on the earlier spectra.[10,11,14,15] (As before, we have used an axis system with the *z* axis perpendicular to the square plane and the *x* axis along the unique ligand–metal bond. The B_1 irreducible representation is defined as the one symmetric to reflection in the *xy* mirror plane.)[14] The lowest energy electric-dipole-allowed, spin-allowed band at 31 300 cm^{-1} is assigned to the $^1A_1 \rightarrow {}^1B_1$, $d_{xy} \rightarrow d_{x^2-y^2}$ transition. The oppositely polarized allowed band at 35 700 cm^{-1} is assigned to the $^1A_1 \rightarrow {}^1B_2$, $d_{xz} \rightarrow d_{x^2-y^2}$ transition.

The intensity of the dipole forbidden, vibronically allowed $^1A_1 \rightarrow {}^1A_2$, $d_{yz} \rightarrow d_{x^2-y^2}$ band is lower than that of the dipole-allowed, spin-allowed transitions. This band overlaps the $^1B_2$ band and appears as a shoulder in the room-temperature spectra and more clearly in the low temperature spectra. In Figure 2, the $^1B_2$ band dominates in the polarization direction shown by the dotted line while the $^1A_2$ band dominates the solid-line spectrum. The changing intensities of these overlapping bands with changes in polarization manifest themselves as an apparent shift in the band maximum.

Calculation of the Transition Energies and the Ligand Field Parameters. The transition energies and the AOM σ- and π-interaction parameters e_σ and e_π are calculated by using the methods described previously.[11,13-15] The parameter set and the number of variables were described in detail.[15] The calculation discussed here uses the minimum number of variables (B, C, e_σ, $e_{\pi_\parallel}$, $e_{\pi_\perp}$) by assuming that the spin–orbit-coupling constant and AOM parameters for the chloride ligands can be transferred between the $PtCl_3L^{n-}$ complexes within a range of 100 and 600 cm^{-1}, respectively. The results of the complete ligand field calculation, which includes spin–orbit coupling, are listed in the Table I. The parameters that were used are given at the end of the table. While the fitting procedure was being performed, it was noted that the $^1B_2$ and $^1A_2$ transitions were very sensitive to the Racah *B* parameter and much less sensitive to the Racah *C* parameter or the spin–orbit coupling. The $^1B_1$ transition was less sensitive to *B* than the other singlet bands and had approximately the same sensitivity to *C* and spin–orbit coupling as the other singlets.

The energies calculated for the singlet transitions are in close agreement with the observed transition energies, with a mean discrepancy of only 100 cm^{-1}. The states that give rise to the calculated transitions are the same as those assigned above, which further supports the band assignments.

The calculated triplet transition energies form clusters of closely spaced components, which are in good agreement with the energies of the observed spin-forbidden bands. The irreducible representations listed in Table I for each of the spin–orbit-coupled components are those with the largest coefficients in the wavefunction.

It is interesting to compare the calculated bonding parameters of the triethylphosphine ligand to those of the previously studied ligands in the $PtCl_3L^{n-}$ series, ethylene,[14] trimethylamine,[15] ammonia,[12] and chloride.[12] Triethylphosphine is a significantly stronger σ donor than any of the above ligands (compare $e_\sigma = 23\,500$ cm^{-1} for triethylphosphine to $e_\sigma = 15\,160$ cm^{-1} for ethylene, $e_\sigma = 21\,700$ cm^{-1} for trimethylamine, and $e_\sigma = 11\,800$ cm^{-1} for chloride). The triethylphosphine ligand is a poorer π donor, (i.e. a better π acceptor) than trimethylamine and chloride and is a better π donor than ethylene. On the basis of the results from the $PtCl_3L^{n-}$ complexes studied to date, the uncertainties in the AOM parameters are about ±600 cm^{-1}. The uncertainty arises partly from the inherent uncertainties in the fitting procedure and partly from the fact that a specific ligand such as chloride would not be expected to have a constant value as L is changed. The difference between the AOM parameters for the ligands studied to date are outside of the uncertainty limits. In summary, the relative position of triethylphosphine in the two-dimensional spectrochemical series for the $PtCl_3L^{n-}$ series is as follows: for σ donors, $PEt_3 > NMe_3 > C_2H_4 > Cl^- > Br^-$; for π donors, $NMe_3 > Cl^- > PEt_3 > C_2H_4$.

Acknowledgment. The authors thank Lee Tutt for preliminary measurements and the National Science Foundation for financial support.

Registry No. $(Pr_4N)[PtCl_3PEt_3]$, 19508-37-3.

Contribution from the Nuclear Research Centre Negev
and Coal Research Center and the Chemistry Department,
Ben-Gurion University of the Negev, Beer-Sheva, Israel

Kinetics of Formation and Decomposition of the Methyl–Copper(II) Complex in Aqueous Solutions. A Pulse-Radiolysis Study

Haim Cohen*† and Dan Meyerstein*‡

Received July 31, 1985

The effect of copper ions on the product composition in catalytic free-radical processes in aqueous solutions was interpreted as indicating that short-lived intermediates with copper–carbon bonds are formed in these processes.[1,2] Recently it was shown that indeed reactions 1 and 2 can be followed in aqueous solutions by

$$Cu^{2+}_{aq} + \cdot R \xrightarrow{k_1} [Cu^{III}\text{–}R]^{2+}_{aq} \qquad (1)$$

$$Cu^{+}_{aq} + \cdot R \xrightarrow{k_2} [Cu^{II}\text{–}R]^{+}_{aq} \qquad (2)$$

using the pulse-radiolysis or flash-photolysis techniques[3–6] (where $\cdot R$ is an aliphatic free radical). These techniques enable also the study of the properties of the $[Cu^{III}\text{–}R]^{2+}_{aq}$ and $[Cu^{II}\text{–}R]^{+}_{aq}$ complexes.

In all the systems where reaction 2 was studied, the cuprous ions were prepared in situ by the pulse or flash. The study of reaction 2 was therefore limited to free radicals for which reaction 1 is relatively slow, i.e. $k_1 < 1 \times 10^8\ M^{-1}\ s^{-1}$, and preferably to systems for which the transient $[Cu^{III}\text{–}R]^{2+}_{aq}$ is extremely short lived; i.e., $t_{1/2} < 1\ \mu s$.[3] We wish to report here that one can overcome these limitations by preparing solutions of Cu^{+}_{aq} via

$$Cu^{2+}_{aq} + Cr^{2+}_{aq} \rightarrow Cu^{+}_{aq} + Cr^{III}_{aq} \qquad (3)$$

By use of this reaction, solutions containing $[Cu^{+}_{aq}]/[Cu^{2+}_{aq}] \leq 0.2$ can be easily prepared and kept for several hours.[7] As k_2 is in many systems over two-orders of magnitude larger than k_1, reaction (2) can be directly followed. (The reactions of Cr^{III}_{aq} with aliphatic free radicals are very slow.)[8]

As the methyl radical is the simplest aliphatic free radical and the properties of other free radicals are compared to it, we decided to study the reaction

$$Cu^{+}_{aq} + \cdot CH_3 \rightarrow [Cu^{II}\text{–}CH_3]^{+}_{aq} \qquad (4)$$

The corresponding reaction with Cu^{2+}_{aq} is extremely slow.[5] The properties of $[Cu^{II}\text{–}CH_3]^{+}_{aq}$ were earlier studied applying the flash-photolytic technique.[5] However the limitations of the technique did not enable a detailed kinetic study or product analysis.

Nitrous oxide saturated solutions containing $(5\text{–}30) \times 10^{-4}$ M $CuSO_4$, $(2\text{–}20) \times 10^{-5}$ M, Cr^{III}_{aq} and Cu^{+}_{aq}, and 0.1–1.0 M $(CH_3)_2SO$ in the pH range 0.7–5.0 were irradiated by 0.3–1.5 μs pulses of 200-mA 5-MeV electrons. The experimental setup was identical with that described earlier in detail.[3] The pulse intensity was 800–3000 rad. At pH $\geq$3.0 the following reactions as well as reaction 4[12] have to be considered:

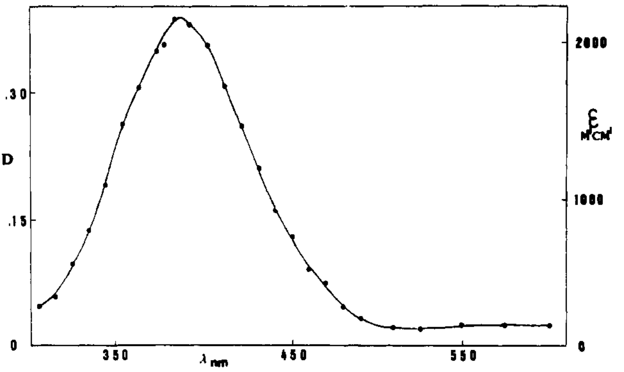

Figure 1. Spectrum of $CuCH_3{}^{+}_{aq}$ measured 10 μs after the pulse: N_2O-saturated solution containing 9×10^{-4} M $CuSO_4$, 2×10^{-4} M $Cr_{aq}{}^{2+}$, and 0.09 M $(CH_3)_2SO$ at pH 3.9; pulse intensity 1500 rad/pulse.

$$H_2O \xrightarrow{e^-} e_{aq}^-, \cdot OH, \cdot H, H_2, H_2O_2, H_3O^+_{aq} \qquad (5)$$

$$e_{aq}^- + N_2O \xrightarrow{H_2O} \cdot OH + OH^-_{aq} + N_2 \qquad k = 8.7 \times 10^9\ M^{-1}\ s^{-1}\ \text{[9]} \qquad (6)$$

$$e_{aq}^- + Cu^{2+}_{aq} \rightarrow Cu^{+}_{aq} \qquad k = 3.1 \times 10^{10}\ M^{-1}\ s^{-1}\ \text{[9]} \qquad (7)$$

$$\cdot H + Cu^{+}_{aq} \rightarrow CuH^{+}_{aq} \qquad 5 \times 10^9 < k < 2 \times 10^{10}\ M^{-1}\ s^{-1}\ \text{[10]} \qquad (8)$$

$$CuH^{+}_{aq} \xrightarrow{H_2O} Cu^{2+}_{aq} + H_2 + OH^-_{aq} \qquad k = 4 \times 10^3\ s^{-1}\ \text{[10]} \qquad (9)$$

$$\cdot OH + (CH_3)_2SO \rightarrow \cdot CH_3 + CH_3SOOH \qquad k = 7.0 \times 10^9\ M^{-1}\ s^{-1}\ \text{[11]} \qquad (10)$$

In more acidic solutions reaction 11 competes with reactions 6 and 7.

$$e_{aq}^- + H_3O^+ \rightarrow \cdot H \qquad k = 2.0 \times 10^{10}\ M^{-1}\ s^{-1}\ \text{[9]} \qquad (11)$$

Under these conditions one might expect a competition between reaction 8 and reaction 12.

$$H\cdot + (CH_3)_2SO \rightarrow (CH_3)_2\dot{S}OH \xrightarrow{H_3O^+} (CH_3)_2S^{\cdot +} + H_2O \qquad (12)$$

The latter reaction has been observed only in strong acidic solutions.[13] We have not detected under our experimental conditions

---

† Nuclear Research Centre Negev and Coal Research Center.

‡ Chemistry Department.

(1) Kochi, J. K. *Acc. Chem. Res.* **1974**, *7*, 351. *Free Radicals*; Kochi, J. K., Ed.; Wiley: New York, 1973; Vol. 1, Chapter 11.

(2) Walling, C. *Acc. Chem. Res.* **1975**, *8*, 125. Walling C.; Kats, S. *J. Am. Chem. Soc.* **1971**, *93*, 4275.

(3) Freiberg, M.; Meyerstein, D. *J. Chem. Soc., Chem. Commun.* **1977**, 934; *J. Chem. Soc., Faraday Trans. 1* **1980**, *76*, 1825, 1838.

(4) Buxton, G. V.; Green, J. C.; Sellers, R. M. *J. Chem. Soc., Dalton Trans.* **1976**, 2160 and Buxton, G. V.; Green, J. C. *J. Chem. Soc., Faraday Trans. 1* **1978**, *74*, 697.

(5) Ferraudi, G. *Inorg. Chem.* **1978**, *17*, 2506.

(6) Das, S.; Johnson, J. R. *J. Chem. Soc., Faraday Trans. 1* **1980**, *74*, 1779.

(7) Shaw, K.; Espenson, J. H. *Inorg. Chem.* **1968**, *7*, 1619.

(8) Meyerstein, D. Ph.D. Thesis, The Hebrew University of Jerusalem, 1965.

(9) Anbar, M.; Bambenck, M.; Ross, A. B. *Natl. Stand. Ref. Data Ser.* (*U.S., Natl. Bur. Stand.*) **1973**, *NSRDS-NBS 43*.

(10) Mulac, W. A.; Meyerstein, D. *Inorg. Chem.* **1982**, *21*, 1782.

(11) Veitwisch, D.; Janata, E.; Asmus, K. D. *J. Chem. Soc., Perkin Trans. 2* **1980**, 146.

(12) The reactions of free radicals, except e_{aq}^-, with $Cr(III)_{aq}$ are known to be very slow[8] and are therefore not considered.

(13) Chaudhri, S. A.; Goelb, M.; Freyholdt, T.; Asmus, K. D. *J. Am. Chem. Soc.* **1984**, *106*, 5988.

0020-1669/86/1325-1505$01.50/0 © 1986 American Chemical Society